Fluctuations in the unimolecular decomposition of jetcooled NO2: Implications for overlapping resonances and the transition state

S. A. Reid, D. C. Robie, and H. Reisler

Citation: The Journal of Chemical Physics **100**, 4256 (1994); doi: 10.1063/1.466308
View online: http://dx.doi.org/10.1063/1.466308
View Table of Contents: http://scitation.aip.org/content/aip/journal/jcp/100/6?ver=pdfcov
Published by the AIP Publishing

Fluctuations in the unimolecular decomposition of jet-cooled NO_2: Implications for overlapping resonances and the transition state

S. A. Reid, D. C. Robie,[a] and H. Reisler
Department of Chemistry, University of Southern California, Los Angeles, California 90089-0482

(Received 23 August 1993; accepted 3 December 1993)

We report a detailed examination of fluctuations in the internal state distributions of the NO ($^2\Pi$) fragment formed in the monoenergetic unimolecular decomposition of jet-cooled NO_2, utilizing photofragment yield (PHOFRY) spectroscopy. The NO(v,J,Ω,Λ) PHOFRY spectra at $E^\dagger < 3000$ cm^{-1} are highly structured, and we examine correlations among these spectra on the basis of the angular momentum, spin–orbit, parity, and vibrational labels of the monitored NO rovibrational levels. We find that levels of similar total angular momentum in the same vibrational manifold are more strongly correlated with specific resonances in the activated molecule, as well as levels of the same N in the two spin–orbit states of NO. The observed PHOFRY correlations, as well as those found in the NO($^2\Pi_\Omega$; $\Omega=1/2,3/2$) rotational state distributions, are interpreted in terms of projections of coherently excited overlapping molecular eigenstates onto the manifold of final states via levels of the transition state. The implications of the results to the transition state and the adiabatic evolution of the NO degrees of freedom are discussed.

I. INTRODUCTION

In recent years, increasingly detailed experimental measures of product state distributions for unimolecular dissociations at well-defined energies and angular momenta have provided stringent tests of statistical theories.[1–3] For dissociations proceeding without a barrier, phase space theory (PST) has proven successful in modeling product rotational state distributions.[1,2] However, PST is less successful in describing product vibrational state distributions and decomposition rates.[1,2,4] The reason for this is clear: The PST transition state (TS) is set at infinite product separation (i.e., PST assumes a very "loose" TS).[5] Since free exchange of energy between the degrees of freedom correlating to product rotation and translation is expected to occur until product separation, the rotational TS is indeed loose. However, the vibrational TS is in general "tighter" than that of rotation since the product vibrations inherently arise from an ensemble of parent *vibrational* degrees of freedom.[1,2] The notion of separate transition states is supported by the relative inefficiency of vibrational vs rotational energy transfer in bimolecular collisions.[6] To correct for the deficiencies of PST in estimating vibrational state distributions, the separate statistical ensembles (SSE/PST) method[7] and variational Rice–Ramsperger–Kassel–Marcus (RRKM) theory[8] have been proposed, and both have proven successful in modeling product vibrational state distributions for several unimolecular decompositions.[1,2,7,9]

In previous publications,[10,11] we reported the application of PST and SSE/PST to model, respectively, the rotational and vibrational state distributions of the NO($^2\Pi_\Omega$; $\Omega=1/2,3/2$) fragment from the monoenergetic unimolecular decomposition of NO_2 at excess energies $E^\dagger=0$–3038 cm^{-1}. In those studies, we found the NO rotational state distributions to be well fit *on average* by PST, although significant fluctuations and oscillations were observed about the PST predictions. In contrast, the vibrational state distributions were consistently "hotter" than predicted by PST, even when taking into account the observed nonstatistical spin–orbit state distributions of O($^3P_{j=2,1,0}$) (Ref. 12) and NO($^2\Pi_\Omega$; $\Omega=1/2,3/2$).[11] The SSE/PST method, employed by treating the parent bending motion either as an unhindered rotor or as a low frequency bend at the TS, gave upper and lower bounds, respectively, for the NO($v=1$)/($v=0$) ratio in the excess energy region $E^\dagger=1900$–3038 cm^{-1}.

Evidence for the statistical nature of the unimolecular reaction of NO_2 is also provided by rate measurements, which are in good agreement with statistical predictions.[13–15] The decomposition rates [$k(E)$] in the range $E^\dagger=0$–1500 cm^{-1} have recently been determined by Wittig and co-workers both at 300 and 5 K using subpicosecond time-resolved measurements,[13] and found to be in accord with the indirect measurements of Troe and co-workers[14] and with RRKM predictions. An intriguing result of this work is the observation of a step-like dependence of $k(E)$ vs $E^\dagger$ near threshold in experiments employing jet-cooled samples. Very recent calculations[15] using variational RRKM theory and cuts in the potential energy surface (PES) in the region near the TS give reasonable agreement with the rate measurements,[13] and fit well, on average, our experimental vibrational distributions,[11] although significant fluctuations are observed about the statistical expectation.

With vibronic state density $\rho_{vib} < 1$ per cm^{-1} near dissociation threshold [$D_0=25\,130\pm2$ cm^{-1} (Refs. 16–18)], it might appear that NO_2 represents a prototypical system exhibiting restricted IVR. However, there is a strong nonadiabatic interaction via the asymmetric stretching mode which results in a conical intersection of the excited $^2B_2$

[a]Present address: Department of Chemistry, Barnard College, New York, NY 10027-6598.

 0021-9606/94/100(6)/4256/16/$6.00

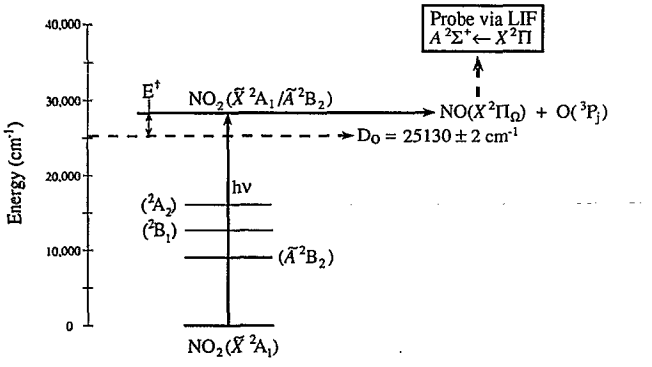

FIG. 1. An energy level diagram of NO_2. Single photon excitation from the ground $^2A_1$ state prepares eigenstates of predominantly ($^2B_2/^2A_1$) character, which are optically accessed via the allowed ($^2B_2 \leftarrow ^2A_1$) transition.

and ground $^2A_1$ surfaces near the $^2B_2$ minimum, giving rise to the extreme complexity of the NO_2 visible absorption spectrum.[19–23] The effects of this nonadiabatic interaction extend to dissociation threshold, and indeed, vibronic chaos is evident in NO_2 at energies $>16\,000\ cm^{-1}$.[22,23] The mode composition of eigenstates closer to D_0, where the increased importance of spin–orbit and Coriolis couplings destroy the goodness of vibronic symmetry labels, has been recently examined by Delon *et al.*[22] confirming the chaotic nature of the strongly mixed $^2B_2/^2A_1$ eigenstates.[20–29] We note that in addition to the $^2B_2$ state, there are two additional electronic states ($^2B_1$ and $^2A_2$) with origins well below dissociation threshold,[24–27] however, it has been shown that eigenstates in the vicinity of D_0 are predominantly of $^2B_2/^2A_1$ character, and each molecular eigenstate can be described as a linear combination of many zeroth-order ground state wave functions with random coefficients.[20–29] A schematic of the dissociation mechanism of NO_2 which summarizes the known spectroscopic information is shown in Fig. 1.

As mentioned previously, the NO rotational and vibrational state distributions from the unimolecular decomposition of NO_2 at $E^\dagger = 0$–$3038\ cm^{-1}$ are well fit *on average* by the statistical predictions of PST and variational RRKM theory, respectively, although in each case, significant fluctuations about the statistical expectation are observed. These fluctuations, first observed by Robra *et al.* just above D_0,[16] persist even at $E^\dagger = 3038\ cm^{-1}$.[11] We interpret them as arising from the coherent excitation of overlapping resonances and their projection onto final product states via the transition state.[10,11] In this report, we concentrate on these fluctuations in an attempt to extract more information regarding the statistical nature of and dynamical effects in the photoinitiated unimolecular decomposition of NO_2, a simple bond-fission reaction that proceeds without a barrier. We note that, in addition to NO_2, fluctuations of this type have been observed in the photodissociation of another triatomic molecule, CO_2.[30] In this case, fluctuations observed in the CO rotational distributions following photodissociation at 157.6 nm, $CO_2 \rightarrow CO\ (X\,^1\Sigma) + O(^1D)$, are similar to those observed in NO_2, while the CO $v=0$ and 1 rotational distributions are well described on average by PST.[10] Fluctuations were also observed in the two-photon dissociation of NO_2 to $NO(^2\Pi) + O(^1D)$.[31]

Fluctuations in unimolecular decay rates have been seen in an elegant and detailed series of experiments on formaldehyde, a molecule that dissociates over a large barrier via a tight TS.[32–36] Using Stark level-crossing spectroscopy,[33] the fluorescence lifetimes of selected *J,K,M*-resolved S_1 rovibronic eigenstates were monitored as the states were Stark tuned across metastable S_0 states, providing eigenstate-resolved unimolecular decay rates. The observed rates and S_0–S_1 coupling matrix elements varied by over two orders of magnitude for eigenstates differing in energy by fractions of cm^{-1}. In addition, some asymmetric line shapes were observed in Stark level-crossing spectra of D_2CO, and were interpreted as the manifestation of interference effects due to dissociation through overlapping S_0 resonances coupled to the same set of continuum states.[35] More recently, fluctuations in the CO rotational state distributions have been observed at higher excess energies and shown to arise from projection of several excited S_0 resonances onto the final state manifold via the vibrational levels of the tight TS.[36] In this case, the decomposition rates are well described *on average* by the RRKM theory,[32] while product distributions are determined by the exit–channel interactions beyond the barrier.[36]

The observation of fluctuations in reactions proceeding via a compound nucleus is a common phenomenon in nuclear physics.[37–40] In fact, fluctuations in product state populations were predicted by Ericson before they were observed experimentally[40] and are commonly referred to as "Ericson fluctuations."[37,39] They arise from the coherent excitation of overlapping resonances in the compound nucleus and are expected when the density of final states is small and the excitation energy is well defined.

In the field of unimolecular reactions, for which the concepts of an activated molecule and a TS are central precepts of transition state theories,[41] it has long been recognized that resonance-scattering theory may be used to describe reaction rates.[42,43] The resonances in S-matrix theory correspond exactly to states of the activated complex in transition state theories. Most rigorous treatments have either assumed that states of the activated complex do not overlap,[43] or an average over the interferences is taken to obtain the statistical outcome.[44] For example, Mies and Krauss have shown that the common expression for thermal unimolecular reaction rates as described by traditional statistical theories can be obtained when starting from the theory of overlapping resonances and averaging out the interference effects.[44] An average over the interferences is justified when the number of initial levels is large (e.g., in room temperature experiments) and the number of accessible final states is also large. However, when the experimental averaging is minimized (e.g., for a small set of initial states, few final states and monoenergetic excitation), effects due to these interferences may be manifest. Our experiments fall into this latter category.

In this paper, we examine more closely fluctuations in

the NO rotational distributions and their implications to the statistical description of the decomposition. Preliminary results utilizing both one-photon and double-resonance infrared/visible photofragment yield (PHOFRY) spectra have recently been reported[45] and show a marked sensitivity of the spectra to the monitored NO state. We report here detailed rotational state distributions and one-photon photofragment yield (PHOFRY) spectra which allow comparisons among the partial cross sections for formation of NO in specific rovibrational (v,J), spin–orbit (Ω), and Λ-doublet states and probe in more depth the correlations previously observed.[11,45] The outline of the paper is as follows: Sec. II briefly describes the experimental techniques used to obtain NO($^2\Pi$) product state distributions and PHOFRY spectra. In Sec. III, we present the main results of this work, which consist of (1) the correlation observed among fluctuation patterns in the rotational distributions obtained for separate NO Λ-doublet states; (2) the strong correlation among rotational state distributions in the NO $^2\Pi_{1/2}$, $^2\Pi_{3/2}$ spin–orbit manifolds; and (3) correlations among PHOFRY spectra sorted by total angular momentum, electronic parity, total parity, spin–orbit and the vibrational state labels of the monitored NO rovibrational levels. Section IV discusses the results within the framework of statistical theories in terms of overlapping resonances, vibrational levels of the TS, decomposition rates, and the evolution of the different NO degrees of freedom via the TS.

II. EXPERIMENTAL METHOD

The experimental apparatus and methodologies have been previously discussed in detail.[11,46] Briefly, an equal mixture of NO_2/O_2 in He (typically 1%–5%) at total pressures of 600–760 Torr is expanded into an octagonal vacuum chamber (base pressure 2×10^{-6} Torr) using a piezoelectrically actuated pulsed nozzle (0.5 mm diam. orifice, 180 μs pulse width). The free jet is crossed $\sim$15 mm downstream of the orifice at 90° by collinear and counter-propagating photolysis and probe laser beams, each generated by separate excimer pumped tunable dye laser systems. The photolysis and probe beams are linearly polarized in a direction orthogonal to the axis of the detector. For photolysis, tunable radiation in the range $\lambda=398$–358 nm is generated using the dyes QUI (398–370 nm) and BPBD-365 (373–358 nm). Typical pulse energies are 3–9 mJ in a 3 mm diam. beam. For photolysis at 354.7 nm, the third harmonic of a Nd:YAG laser is used, which has a larger bandwidth than the excimer pumped dye laser system (i.e., $\sim$2 vs $\sim$0.5 cm^{-1}). Probe radiation in the range $\lambda=220$–230 nm is generated by frequency doubling the probe dye laser fundamental (C450, C460) in a BBO crystal. Nascent NO($^2\Pi_{1/2}$,$^2\Pi_{3/2}$;v,J) fragments are detected by one-photon laser induced fluorescence (LIF) on the diagonal bands of the well-known γ system[47] at a typical photolysis-probe delay of 200 ns. The fluorescence is imaged by a three lens telescope through a "solar blind" (Corion, 300 nm, 85 nm bandpass) filter onto a photomultiplier tube (Hamamatsu RU166H), which is oriented at 90° to both the axis of the jet and of the laser beams. The photomultiplier tube (PMT) signal is digitized by a digital storage oscilloscope and recorded by a PC, which controls data acquisition and laser frequency stepping.

Two types of experiments were carried out. In the first arrangement, the photolysis laser frequency was fixed at a specific energy above the NO_2 dissociation threshold in the range $E^\dagger=0$–3038 cm^{-1} and the probe laser frequency then scanned over the (0,0) and (1,1) bands of the γ system. The probe pulse energy was attenuated to <3 μJ ($\sim$5 mm beam diam.) to avoid saturation of the stronger rotational branches of the γ system.[11] Internal state distributions of the NO fragment were obtained by converting the observed LIF intensities to populations in the manner previously described.[11] In the second experimental arrangement, the probe laser frequency was tuned to excite a specific NO rovibrational transition in one spin–orbit manifold and the photolysis laser frequency scanned to obtain the yield spectrum for dissociation into the monitored state, which we term photofragment yield (PHOFRY) spectra. In this arrangement, higher probe pulse energies were used ($\sim$10–40 μJ) since saturation effects were not important.

III. RESULTS

A. Correlation of fluctuations in the rotational state distributions of the NO($^2\Pi_\Omega$; $\Omega=1/2,3/2$) fragment

As an example of the fluctuations observed in NO rotational distributions from the photoinitiated decomposition of NO_2, we show in Fig. 2 NO($^2\Pi_{1/2}$) rotational distributions from NO_2 photolysis at excess energies $E^\dagger=400$, 2061, 2200, and 3038 cm^{-1}, respectively, displayed as Boltzmann plots [i.e., ln(rotational state population/degeneracy) vs rotational energy]. In each figure, the populations of the two Λ-doublet levels (notated A' and A'') for each rotational level are plotted separately, and the error bars, while not shown, are on the order of the symbol size. Also shown in each figure is the distribution predicted by PST, as detailed in a previous article.[11] Prominent fluctuations about the statistical prediction of PST are clearly observed at all $E^\dagger$, and inspection of the fluctuation patterns observed in the separate Λ-doublet level distributions reveal a consistent correlation at the majority of excess energies examined. As a result, summing over the Λ-doublet level populations does not, at most energies, yield a distribution much more consistent with a PST prediction.[11]

The rotational distributions obtained for the two NO spin–orbit states also exhibit pronounced similarities. Examples are shown in Fig. 3, which displays NO($^2\Pi_{1/2}$) and NO($^2\Pi_{3/2}$) rotational distributions at the same excess energies, summed over Λ-doublet levels. Prominent fluctuations in each distribution are observed, yet the fluctuation patterns at each energy are quite similar for the two spin–orbit states. Furthermore, in most cases, the distributions for the $^2\Pi_{3/2}$ state are shifted with respect to the $^2\Pi_{1/2}$ distribution, usually by one rotational quantum to lower J. This observation is particularly evident when comparing the separate Λ-doublet distributions of each spin–orbit

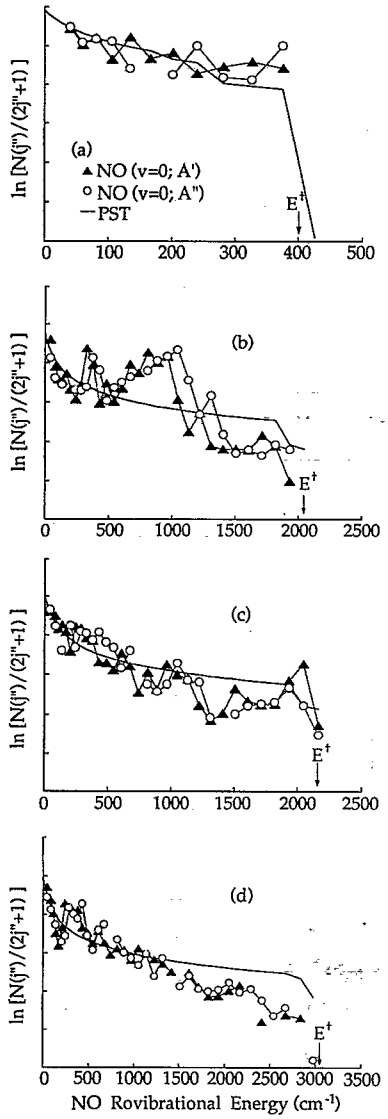

FIG. 2. Boltzmann plots of rotational state distributions of the NO ($^2\Pi_{1/2}$,v=0) fragment following NO_2 photolysis at excess energies (a) $E^\dagger$=400; (b) 2061; (c) 2200; and (d) 3038 cm^{-1}. The corresponding photolysis wavelengths are (a) 391.70; (b) 367.77; (c) 365.90; and (d) 354.7 nm. In each figure, the distributions of the two Λ-doublet levels are plotted separately, and also shown (solid line) is the distribution predicted by phase space theory (PST).

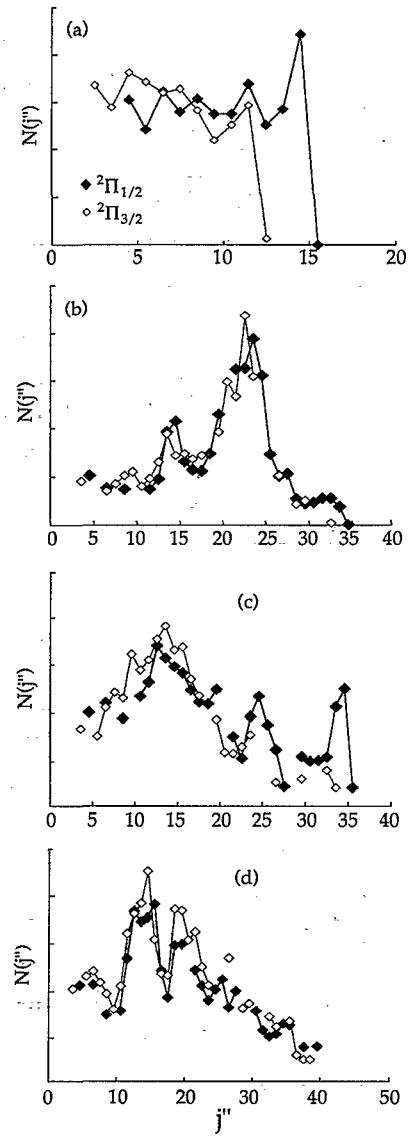

FIG. 3. Rotational state distributions of the NO($^2\Pi_{1/2}$,v=0) and NO($^2\Pi_{3/2}$,v=0) fragments following NO_2 photolysis at excess energies (a) $E^\dagger$=400; (b) 2061; (c) 2200; and (d) 3038 cm^{-1}. In each panel, the distributions for the two Λ-doublet levels are summed. Note the good reproduction of fluctuation patterns in the distributions for the two spin–orbit states.

state (Fig. 4). We note that for the NO $^2\Pi_{1/2}(F_1)$ and $^2\Pi_{3/2}(F_2)$ states, $J=N+1/2$ and $N-1/2$, respectively (N is the sum of the nuclear rotational angular momentum and $\Lambda=1$). The observation of a shift in the rotational distribution of the $^2\Pi_{3/2}$ state by one to lower J thus reflects structures in the distributions which depend similarly on the value of N. It is the good reproduction of the fluctuation patterns in the two spin–orbit manifolds which allows comparison of PHOFRY spectra obtained by monitoring either $^2\Pi_{1/2}$ or $^2\Pi_{3/2}$ rovibronic levels (see below). As shown previously,[11] the total NO($^2\Pi_{1/2}$)/NO($^2\Pi_{3/2}$) ratio is remarkably constant over the full range of excess energies examined, with production of the ground NO($^2\Pi_{1/2}$) state consistently favored by a factor of ~3. We will elaborate on the possible source(s) of this non-statistical spin–orbit state distribution in a later section; however, we note here that this is not an unusual observation. Nonstatistical spin–orbit state populations have been observed in many unimolecular decompositions, even when other level distributions (rotational, vibrational, etc.) are well described by statistical models.[1,48]

A final correlation concerns the rotational distributions for different NO vibrational levels (i.e., v=0 vs v=1).[11] Specifically, at a given excess energy in the range $E^\dagger$=1876–3038 cm^{-1} we observe no correlation in either the presence or structure of fluctuation patterns in the rotational distributions for the two NO vibrational levels. An example is shown in Fig. 5, which displays NO($^2\Pi_{1/2}$) rotational distributions (summed over Λ-doublet levels) and the PST predictions for v=0 and 1, respectively, at $E^\dagger$=2061 cm^{-1}. Prominant fluctuations about the PST av-

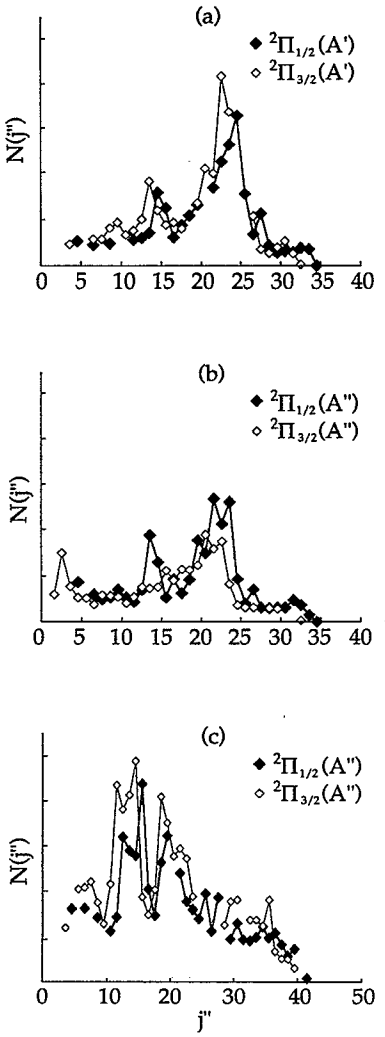

FIG. 4. Rotational state distributions of the $NO(^2\Pi_{1/2},v=0)$ and $NO(^2\Pi_{3/2},v=0)$ fragments following NO_2 photolysis at excess energies ($E^\dagger$) of (a) and (b) 2061; and (c) 3038 cm^{-1}. In this figure, the rotational distributions of the individual Λ-doublet levels of the two spin–orbit states are shown. Note the consistent shift of the $^2\Pi_{3/2}$ distribution with respect to that in the $^2\Pi_{1/2}$ state.

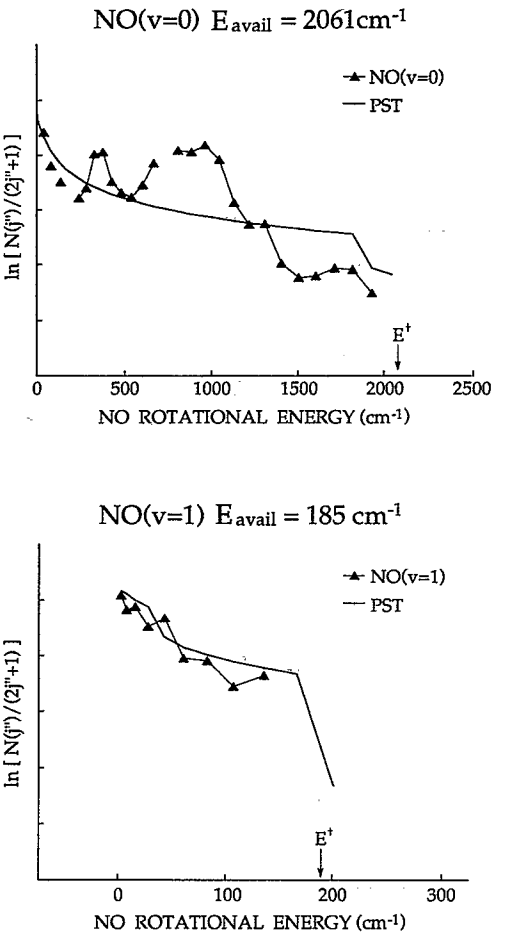

FIG. 5. Rotational state distributions of the $NO(^2\Pi_{1/2},v=0)$ and $NO(^2\Pi_{1/2},v=1)$ fragments following NO_2 photolysis at $E^\dagger$=2061 cm^{-1}, summed over Λ-doublet levels.

erage are clearly observed in the $v=0$ distribution, while the $v=1$ distribution more closely follows the PST prediction. The significance of this observation will be discussed in Sec. IV B.

B. Product state fluctuations as probed by photofragment yield (PHOFRY) spectroscopy

To gain a better understanding of the fluctuations in the NO rotational distributions and further investigate the correlations described above and their dependence on $E^\dagger$, we turned to the examination of PHOFRY spectra. We have previously reported some one-photon[11] and two-photon infrared/visible PHOFRY spectra[45] at $E^\dagger<2800$ cm^{-1}. These spectra are highly structured at all energies, with prominent peaks of 4–100 cm^{-1} full width at half-maximum (FWHM). Representative examples are shown in Fig. 6, which displays two spectra obtained by monitoring NO rovibronic levels in $v=0$ and 1 with similar energy appearance thresholds. Notice that the two spectra are quite different, as was also shown by other workers.[16,49,50] Structured PHOFRY spectra have also been obtained at $E^\dagger$=0–2170 cm^{-1} by monitoring the yield of $O(^3P_j)$ (Ref. 12); however, a marked loss of structure was observed with increasing $E^\dagger$. Miyawaki *et al.* assumed this loss of structure to be due solely to an increase in lifetime broadening as the dissociation time scale decreased with increasing excess energy. However, our NO PHOFRY spectra are still highly structured at $E^\dagger\cong2800$ cm^{-1} (cf. Fig. 6), and other workers have observed structured spectra up to $E^\dagger\approx4500$ cm^{-1}.[50] Moreover, although the dissociation time scale at $E^\dagger=2800$ cm^{-1} is <200 fs, corresponding to a homogeneous lifetime broadening of >25 cm^{-1},[13,14] some narrower features are observed. Since pronounced differences in the NO PHOFRY spectra are observed when monitoring different $NO(v,J)$ levels and each oxygen spin–orbit state *necessarily* correlates with a wide range of $NO(v,J)$ states, the loss of structure observed in the $O(^3P_j)$ PHOFRY spectra is easily understood. In fact, Miyawaki *et al.* have recently shown that near D_0, sum-

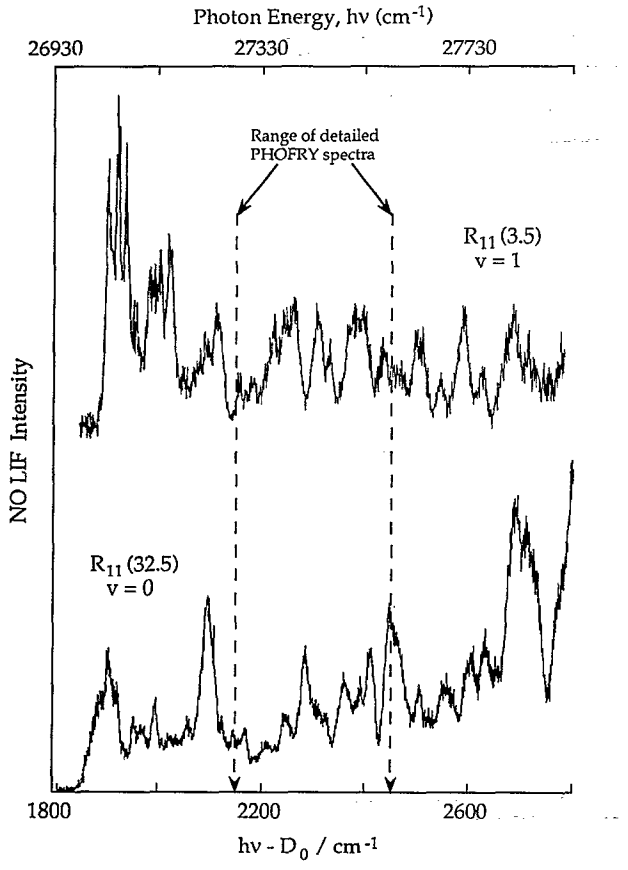

FIG. 6. Photofragment yield (PHOFRY) spectra of NO_2 at $E^{\dagger}=1800$–$2800\ cm^{-1}$ obtained by monitoring the $R_{11}(3.5)$ and $R_{11}(32.5)$ transitions, respectively, of the (1,1) and (0,0) bands of the NO γ system. The energy appearance thresholds for these two levels are similar. Note the degree of structure which persists to $E^{\dagger}=2800\ cm^{-1}$.

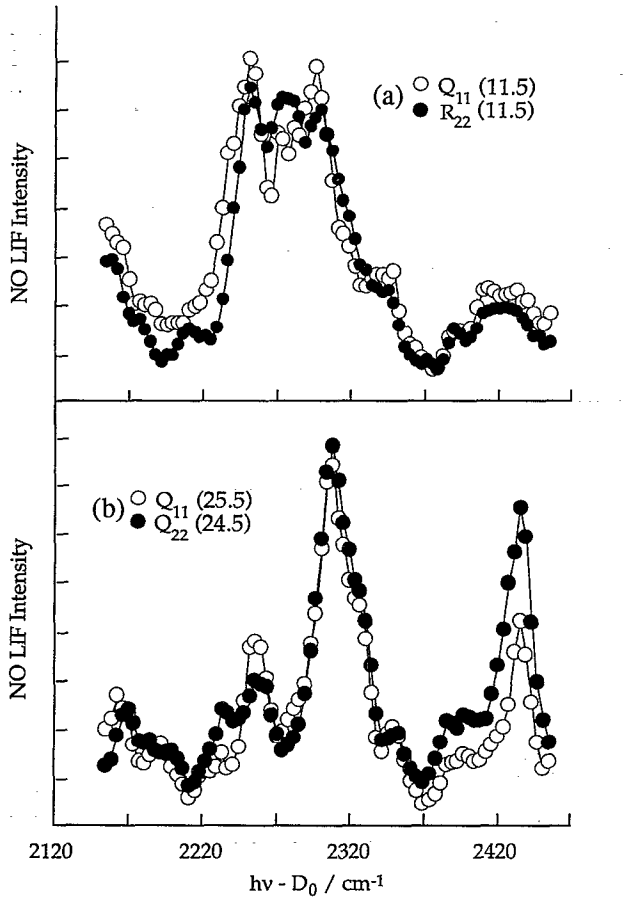

FIG. 7. PHOFRY spectra of NO_2 at $E^{\dagger}=2150$–$2450\ cm^{-1}$ obtained by monitoring (a) the Q_{11} (11.5) and R_{22} (11.5) transitions; and (b) the Q_{11} (25.5) and Q_{22} (24.5) transitions of the NO (0,0) band. These spectra reveal a correlation based on total angular momentum.

ming all the PHOFRY spectra for the populated NO(v,J) states gives a spectrum similar to that obtained by monitoring the yield of $O(^3P_2)$.[49]

For detailed investigation of the nature of the structures observed in the PHOFRY spectra, we concentrated on the region $E^{\dagger}=2150$–$2450\ cm^{-1}$ (see Fig. 6) and obtained a series of PHOFRY spectra by monitoring selected NO rotational levels in the $^2\Pi_{1/2}$ and $^2\Pi_{3/2}$ manifolds of both $v=0$ and 1. To examine correlations among the obtained spectra, we compared them on the basis of Λ-doublet level (electronic parity), total NO parity, and total angular momentum. In addition, we examined PHOFRY spectra of J_{NO} levels both below and above the transition from Hund's case (a) to case (b), which occurs at $\sim J_{NO}=15.5$.[51]

We begin with the more obvious correlations observed in comparing PHOFRY spectra for different NO(v,J) levels. First, as observed at lower $E^{\dagger}$ by utilizing infrared/visible double-resonance PHOFRY spectroscopy,[45] a correlation based on total angular momentum of the monitored NO levels exists. Shown in Figs. 7(a) and 7(b) are pairs of PHOFRY spectra which illustrate that when comparing spectra obtained by monitoring levels of similar total angular momentum, good correlation is seen in the positions and relative intensities of the spectral features. However, noticeable differences are observed when comparing the different pairs of spectra, and thus levels widely separated in rotational quanta (i.e., $J=11.5$ vs 25.5). This result corresponds to the fluctuation patterns obtained in the NO rotational distributions (Figs. 2 and 3 and Ref. 11), which typically exhibit structures of width on the order of several J's. It thus appears that an intrinsic correlation exists between levels of similar total angular momentum and specific resonances in the excited molecule. We should note here that not all PHOFRY spectra for levels of similar total angular momentum display as good a correlation as those shown in Fig. 7, and in some cases, more subtle effects are observed (see below).

The correlations (or lack thereof) of the spectra shown in Fig. 7 are quite obvious; however, such is not always the case, and thus for the remainder of this paper we will employ an index to represent the correlation of specific NO(v,J) PHOFRY spectra based on an autocorrelation analysis. As discussed by Shaw *et al.*,[52] an autocorrelation function $[R(\epsilon)]$ may be defined by the following functional form:

$$R(\epsilon)=\frac{\Gamma^2}{N(\Gamma^2+\epsilon^2)}, \quad (1)$$

where N represents the number of independent final states for a given channel, ϵ is a variable energy increment, and Γ represents the coherence width. We have obtained autocorrelation traces for specific PHOFRY spectra which typically show symmetric Lorentzian-like traces, and in addition are sometimes highly structured. We have not attempted to fit these autocorrelation traces to the functional form of Eq. (1), since, as discussed by Mies,[53] in the case of coherently excited overlapping resonances Γ is not the average decomposition lifetime. As we will later show, the photoinitiated unimolecular reaction of NO_2 in the energy region of these PHOFRY spectra is characterized by coherent excitation of overlapping molecular eigenstates.

We have found that sharp resonance structures are directly reflected as structures on the profiles of the autocorrelation traces. A comparison of the correlation functions for different PHOFRY spectra thus provides a measure of similarities (or differences) in the resonances observed in each spectrum. Following Shaw *et al.*[52] we have chosen to define a normalized correlation index $R_{ij}^N(\epsilon)$ between the PHOFRY spectra obtained when monitoring final states i and j as

$$R_{ij}^N(\epsilon)=\frac{R_{ij}(\epsilon)R_i(\epsilon)}{R_j(\epsilon)R_i(\epsilon)}, \quad (2)$$

where $R_{ij}(\epsilon)$ represents the conventional cross-correlation function for pairs of PHOFRY spectra of levels i,j; and $R_i(\epsilon)$ is the autocorrelation function as previously described. To produce an index which is symmetric about the peak of the correlation function, we have squared the inherently asymmetric cross-correlation function. This index is unity for spectra which are perfectly correlated, but for spectra which exhibit differences in resonance structures, the index fluctuates but is still centered about the ideal value. To illustrate this index, Figs. 8(a) and 8(b) display the correlation indices for the pairs of PHOFRY spectra shown in Figs. 7(a) and 7(b), respectively. As expected, the index for each pair is flat and consistently close to unity. In contrast, a clear lack of correlation is shown in panel 8(c), which compares the spectra of Fig. 7(a) vs 7(b). We emphasize that the label "channel no." of the x axis in Fig. 8 is an arbitrary unitless bin number, which for a single correlation function would represent a specific energy increment, and there is no correlation between the channel number and the location of the x axis in the PHOFRY spectra. We have found this type of correlation index to be insensitive to the exact normalization of the spectra.

For the remainder of this paper, when comparing PHOFRY spectra we will not plot the correlation index, but only give the root-mean-square value of its deviation from unity, i.e.,

$$CI_{rms}=\langle(CI-1)^2\rangle^{1/2}, \quad (3)$$

where CI represents the correlation index for one pair of PHOFRY spectra. The range of CI_{rms} value for the spectra compared in this paper is 0.009–0.098, with the higher

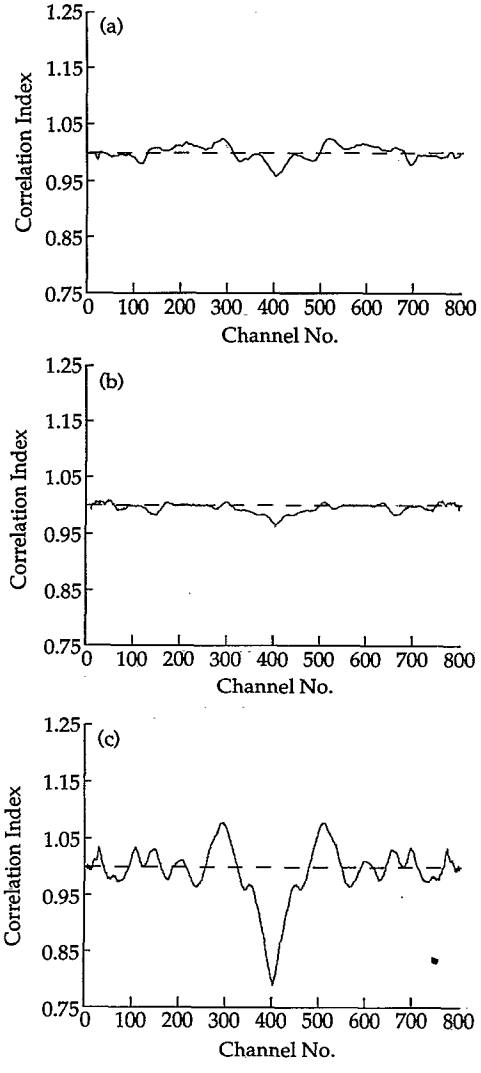

FIG. 8. (a) and (b) Correlation indices for the pairs of PHOFRY spectra shown in Figs. 7(a) and 7(b), respectively, obtained as described in the text. (c) The correlation index of the spectra obtained by monitoring the Q_{11} (11.5) and Q_{11} (25.5) transitions of the NO(0,0) band. The channel number (x axis) is a unitless index which for a single correlation function would represent a specific energy increment. (a) CI_{rms} (see the text) =0.013, (b) 0.009, and (c) 0.058.

values corresponding to more poorly correlated spectra. For example, for those correlation indices shown in Fig. 8(a)–8(c), CI_{rms} values of 0.013, 0.009, and 0.058, respectively, are obtained, which are consistent with the observed correlations, or lack thereof, of the spectra.

In addition to a correlation based on total angular momentum, an important correlation involves NO(v,J) levels in different *vibrational* manifolds (i.e., $v=0$ vs $v=1$).[45] Shown in Fig. 9 is a pair of representative PHOFRY spectra which compare $v=0$ and 1 levels of similar total angular momentum. Much poorer correlation ($CI_{rms}=0.086$) is observed in this comparison than for levels within a single vibrational manifold. As a further check, we examined PHOFRY spectra for rotational levels of $v=0$ and $v=1$ at the same NO rovibrational energy [i.e. ($v=0$, $J=34.5$) vs ($v=1$, $J=10.5$)], which are displayed in Fig. 10. Poor

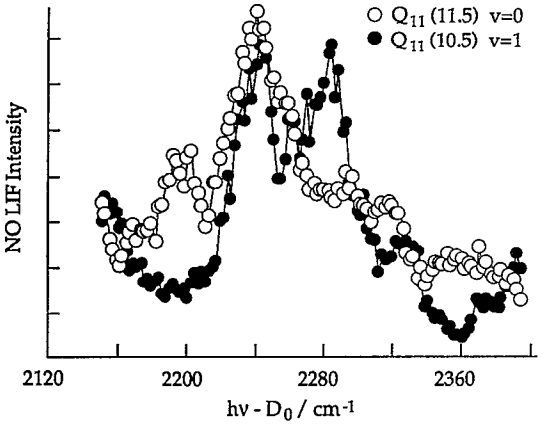

FIG. 9. PHOFRY spectra of NO_2 which compare the Q_{11} (10.5) NO(v=1) spectrum with that obtained by monitoring the Q_{11} (11.5) transition of the NO(0,0) band (CI_{rms}=0.086). These spectra compare levels of similar total angular momentum in separate vibrational manifolds.

correlation (CI_{rms}=0.077) is observed in this comparison, as well as in other spectra of this kind. The weak correlation of the v=0 and v=1 PHOFRY spectra on the basis of either angular momentum or total energy reflects a degree of vibrational adiabaticity indicative of the separate evolution of vibrational and rotational motions in the unimolecular decomposition (see Sec. IV).

We have also observed subtle correlations, based on parity and spin–orbit level, which require more detailed inspection. Welge and co-workers have observed parity oscillations at low $E^{\dagger}$, where only $O(^3P_2)$ is populated.[16] However, at higher energies, each NO fragment can correlate with three $O(^3P_j)$ states, therefore conservation of total parity does not dictate the need for preferential population of levels of a specific parity in NO. Displayed in Figs. 11–13 are pairs of PHOFRY spectra obtained by monitoring NO(v=0) rotational levels in the range J=9.5–11.5. Figure 11 displays three pairs of spectra which compare levels of similar total angular momentum

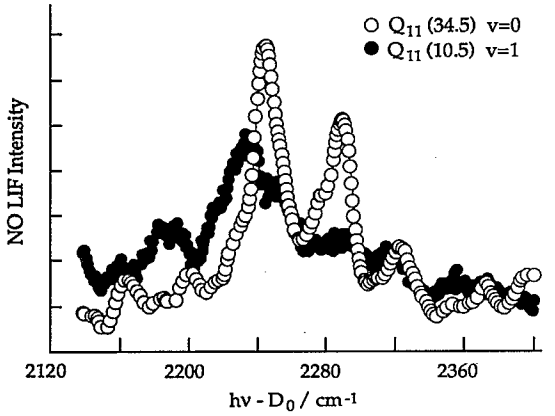

FIG. 10. PHOFRY spectra of NO_2 which compare the Q_{11} (10.5) NO (v=1) spectrum with that obtained by monitoring the Q_{11} (34.5) transition of the NO(0,0) band (CI_{rms}=0.077). These spectra compare levels of similar total rovibrational energy in the separate vibrational manifolds.

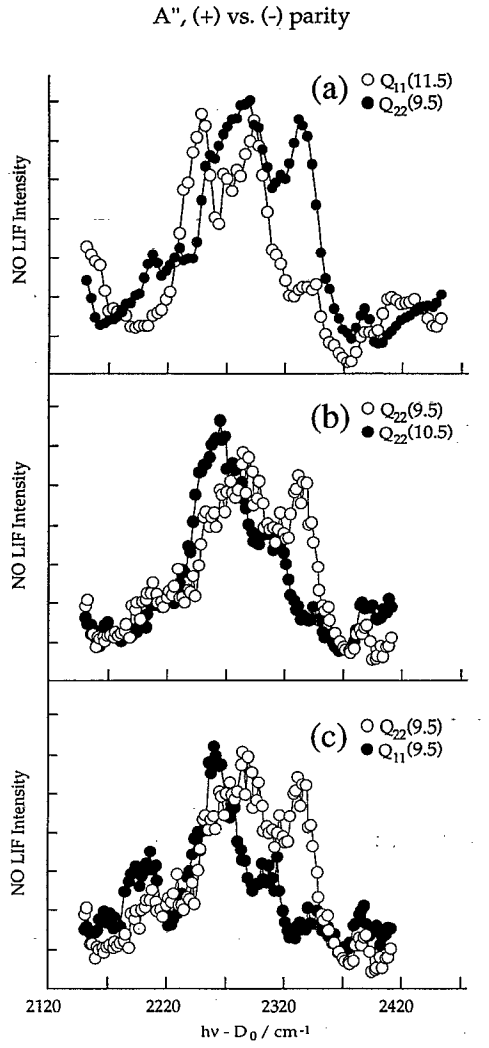

FIG. 11. PHOFRY spectra of NO_2 which compare the spectrum obtained by monitoring the Q_{22} (9.5) transition of the (0,0) band of the NO γ system with those obtained by monitoring (a) the Q_{11} (11.5); (b) the Q_{22} (10.5), and (c) the Q_{11} (9.5) transitions of the same band [(a) CI_{rms}=0.075; (b) 0.062; and (c) 0.057]. These transitions access NO rovibrational levels of similar total angular momentum and the same electronic parity, but different total parity.

and the same electronic parity (i.e., the same Λ-doublet level), but different total parity. CI_{rms} values for these spectra are 0.075, 0.062, and 0.057, respectively. All spectra show a prominent, highly structured feature of width 80–100 cm^{-1} (FWHM), much larger than the expected single resonance width in this energy region of ~20 cm^{-1}.[13,14] In addition, the shape and width of the prominent central feature changes noticeably in the spectra, although certain structures of common origin are clearly discernible.

The correlations of the pairs of PHOFRY spectra displayed in Figs. 11(a)–11(c) should be contrasted with those shown in Figs. 7(a) and 12, which compare NO rovibronic levels of different electronic parity (i.e., different Λ-doublet levels), but the same total parity. These figures show an obvious correlation in the shape of the prominent central feature, which again is highly structured with a width of ~100 cm^{-1} (FWHM). The agreement of the

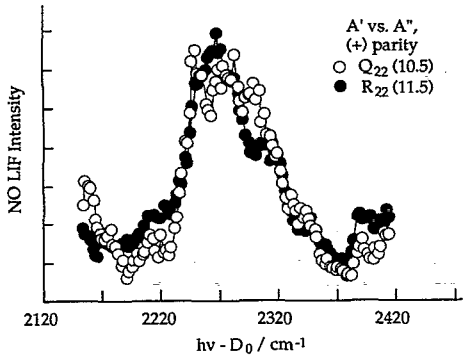

FIG. 12. PHOFRY spectra of NO_2 which compare the spectrum obtained by monitoring the R_{22} (11.5) transition of the (0,0) band of the NO γ system with that obtained by monitoring the Q_{22} (10.5) transition of the same band (CI_{rms}=0.035). These transitions access NO rovibrational levels of similar total angular momentum and the same total parity, but different electronic parity.

relative intensities of the structures within the clump allows for an almost perfect superposition of the spectra in each pair, reflected in small CI_{rms} values of 0.013 [Fig. 7(a)] and 0.035 (Fig. 12). This good agreement is independent of whether the compared levels are in the same or different spin–orbit manifolds, consistent with the pronounced similarity of the rotational distributions for the two spin–orbit states.[11] From a comparison of Fig. 11 with Figs. 7(a) and 12, it appears that better correlation is observed on the basis of total rather than electronic parity of the monitored NO levels.

To continue comparisons based on parity, displayed in Figs. 13(a)–13(c) are three pairs of spectra obtained by monitoring levels of the *same* electronic and total parity. CI_{rms} values for these spectra are 0.032, 0.026, and 0.074, respectively. These spectra exhibit a prominent central feature which in the Q_{22}(10.5) PHOFRY spectrum is clearly resolved into at least two peaks [Fig. 13(b)], and may be compared with the pair shown in Fig. 14, which compares spectra for levels of *different* electronic and total parity (CI_{rms}=0.098). No firm conclusions can be drawn from these spectra regarding possible correlations based on parity.

In a similar manner, we examined correlations in NO(v=0,J) PHOFRY spectra in the range J_{NO}=24.5–26.5, above the transition to Hund's case (b). In the case (b) limit, each Λ-doublet level corresponds to a preferred orientation of the electron density of the lone π electron with respect to the plane of nuclear rotation.[51] The observation of a nonstatistical Λ-doublet level distribution can, for a fast dissociation from a planar transition state, reveal detailed stereochemical information.[51] However, in the NO rotational distributions there is no obvious and consistent bias favoring a particular Λ-doublet level,[11] an observation we wished to examine further by inspecting PHOFRY spectra of levels of differing Λ-doublet origin in the case (b) limit.

Figures 7(b) and 15–18 each display pairs of PHOFRY spectra and their corresponding correlation indices

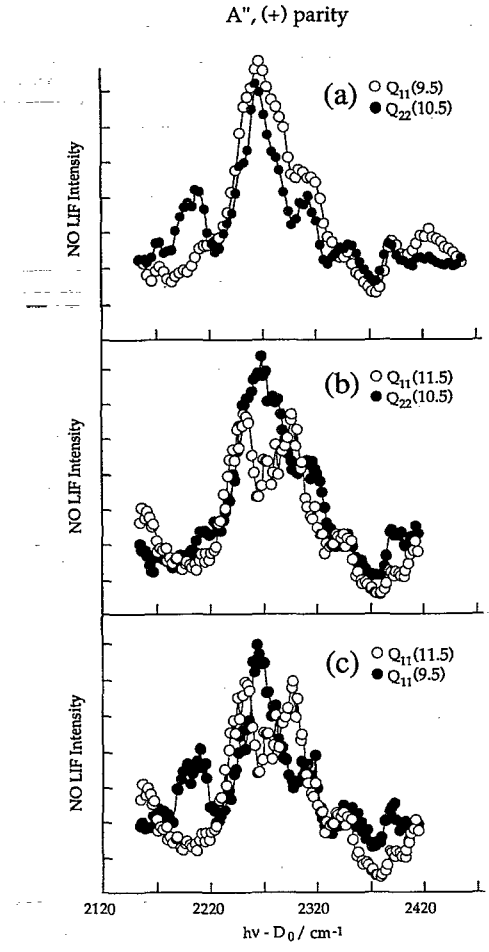

FIG. 13. PHOFRY spectra of NO_2 obtained by monitoring (a) the Q_{11} (9.5) and Q_{22} (10.5) transitions; (b) the Q_{11} (11.5) and Q_{22} (10.5) transitions; and (c) the Q_{11} (11.5) and Q_{11} (9.5) transitions of the (0,0) band of the NO γ system [(a) CI_{rms}=0.032; (b) 0.026; and (c) 0.074]. These transitions access NO rovibrational levels of the same electronic and total parity.

obtained by monitoring NO(v=0, J=24.5–26.5) in both the $^2\Pi_{1/2}$ and $^2\Pi_{3/2}$ manifolds. Figure 15 displays such a pair obtained by monitoring levels of the same total parity, but different electronic parity (Λ-doublet level). In each spectrum, prominent features are observed which are well reproduced, with the largest peak occurring at $E^\dagger \sim 2310$ cm^{-1}. This feature is quite narrow (FWHM$\sim$20 cm^{-1}), yet obviously asymmetric. Following the result obtained from the lower J_{NO} PHOFRY spectra, we may compare Fig. 15 with Fig. 16, which displays a pair of PHOFRY spectra accessing levels of the same electronic parity (the same Λ-doublet level), but different total parity. Again, several intense features are observed, with the largest occurring at $E^\dagger \sim 2310$ cm^{-1} and clearly resolved in the R_{11}(25.5) PHOFRY spectrum as two features. Unlike the lower J_{NO} spectra [e.g., Figs. 7(a), 11, and 12], the correlation of these spectra (CI_{rms}=0.049) is not dramatically different from that of those shown in Fig. 15 (CI_{rms} =0.033).

The spectra shown in Fig. 7(b) were obtained by mon-

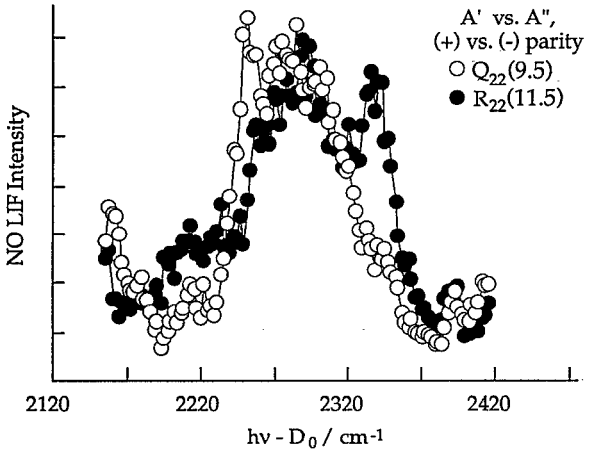

FIG. 14. PHOFRY spectra of NO_2 obtained by monitoring the Q_{22} (9.5) and R_{22} (11.5) transitions of the (0,0) band of the NO γ system (CI_{rms} =0.098). These transitions access NO rovibrational levels of different electronic and total parity.

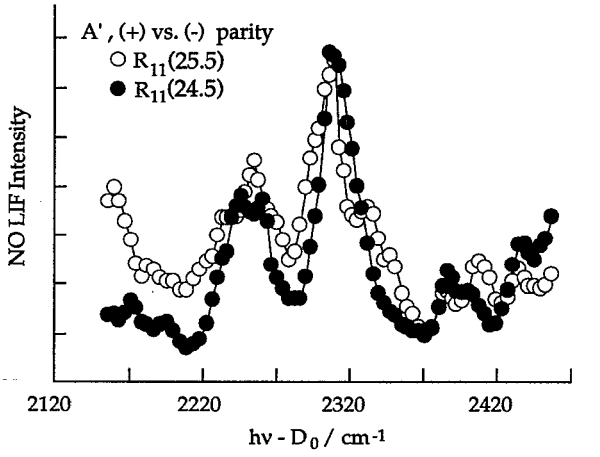

FIG. 16. PHOFRY spectra of NO_2 obtained by monitoring the R_{11} (25.5) and R_{11} (24.5) transitions of the (0,0) band of the NO γ system (CI_{rms}=0.049). These transitions access NO rovibrational levels of the same electronic, but different total parity.

itoring levels of the *same* electronic and total parity (CI_{rms} =0.009), while Fig. 17 displays two spectra obtained by monitoring levels of *different* electronic and total parity (CI_{rms}=0.021). It is important to note that all of the PHOFRY spectra displayed in Figs. 7(b) and 15–17 have features in common. Nevertheless, it is apparent that the best correlation is observed for the pair of spectra shown in Fig. 7(b), which almost identically reproduce the widths and shapes of the observed structures, if not relative intensities. To explain this observation, we remember that as previously mentioned, the rotational distributions of the $^2\Pi_{1/2}$ and $^2\Pi_{3/2}$ spin–orbit states at a given excess energy exhibit remarkable similarity; with a consistent shift observed of the $^2\Pi_{3/2}$ distribution, usually by one quantum to lower J (Fig. 4). This suggests the existence of a $^2\Pi_{1/2}(J)$, $^2\Pi_{3/2}(J-1)$ correlation (i.e., a direct correlation based on N), which should be observable also in the PHOFRY spectra and might explain the good correlation of the spectra shown in Fig. 7(b). To examine this possibility, we obtained, by monitoring the $Q_{11}(J=25.5; N=25)$ and $Q_{22}(J=26.5; N=27)$ (i.e., $\Delta J=+1$; $\Delta N=2$) transitions of the NO(0,0) band, the pair of spectra shown in Fig. 18. Like the spectra shown in Fig. 7(b), these transitions access levels of the same total and electronic parity. However, a comparison of these PHOFRY spectra reveals noticeable differences in the widths, shapes, and positions of several of the observed features, particularly in the energy region $E^{\dagger}\sim$2170–2370 cm^{-1}. It is apparent that the correlation of these spectra (CI_{rms}=0.029) is not as good as that of those shown in Fig. 7(b) (CI_{rms}=0.009), suggesting that the $^2\Pi_{1/2}(J)$, $^2\Pi_{3/2}(J-1)$ correlation observed in the rotational distributions is also evidenced in PHOFRY spectra.

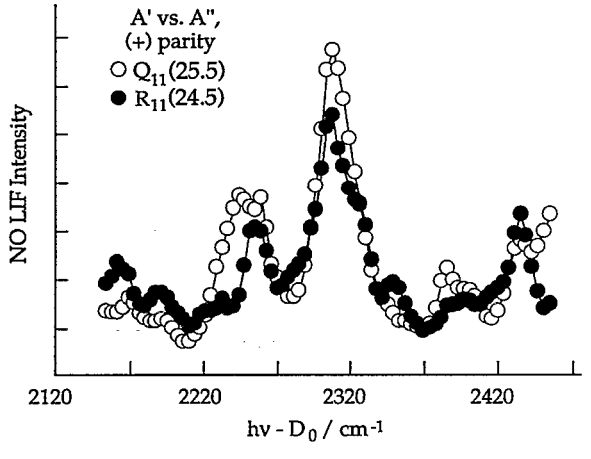

FIG. 15. PHOFRY spectra of NO_2 obtained by monitoring the Q_{11} (25.5) and R_{11} (24.5) transitions of the (0,0) band of the NO γ system (CI_{rms}=0.033). These transitions access NO rovibrational levels of the same total parity, but different electronic parity.

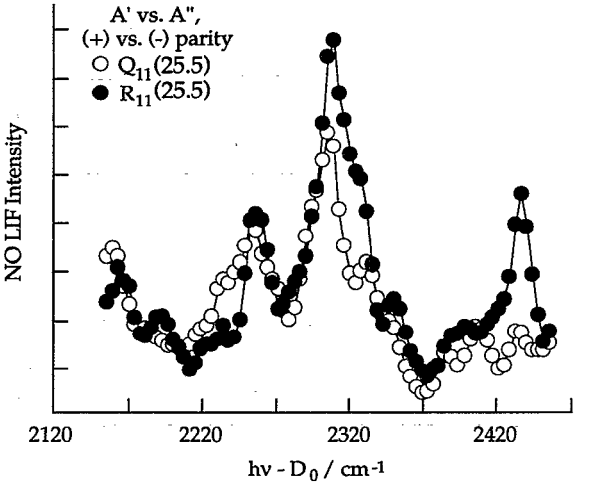

FIG. 17. PHOFRY spectra of NO_2 obtained by monitoring the Q_{11} (25.5) and R_{11} (25.5) transitions of the (0,0) band of the NO γ system (CI_{rms}=0.021). These transitions access NO rovibrational levels of different electronic and total parity.

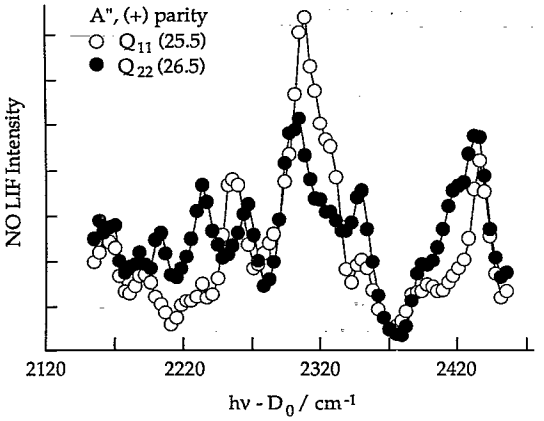

FIG. 18. PHOFRY spectra of NO_2 obtained by monitoring the Q_{11} (25.5) and Q_{22} (26.5) transitions of the (0,0) band of the NO γ system (CI_{rms}=0.029). These transitions access NO rovibrational levels of the same electronic and total parity.

To summarize the results obtained from the NO(v,J) PHOFRY spectra, strong correlations are observed for NO rovibronic levels of similar total angular momenta in the same vibrational manifold. Within these correlations, it appears that at lower J_{NO}, better correlation is observed for spectra of levels of different electronic parity (i.e., different Λ-doublet levels) and the same total parity than for levels of the same electronic and different total parity. This effect is not observed in the higher J_{NO} PHOFRY spectra, and we have not seen such effects in double-resonance PHOFRY spectra obtained at lower $E^{\dagger}$.[45] This observation may therefore be fortuitous. For the higher J_{NO} PHOFRY spectra, the best correlation is observed for $^2\Pi_{1/2}(J)$, $^2\Pi_{3/2}(J-1)$ [i.e., the same N) pairs of levels, reflecting the strong similarity of the rotational distributions for the two spin–orbit states.

IV. DISCUSSION

A. The existence of overlapping resonances and the origin of linewidths in the photofragment yield spectra

We may describe the photoinitiated unimolecular reaction of NO_2 as occurring via the following sequence of events:

$$NO_2(A_1,J_0'',P)+h\nu \rightarrow NO_2^{\dagger}(A_2,J_0',P') \rightarrow NO_2^{\ddagger} \rightarrow NO(^2\Pi_{\Omega};\Omega=1/2,3/2) + O(^3P_j;j=2,1,0),$$

where $NO_2^{\dagger}(A_2,J_0',P')$ is a rovibronic state of mixed $\tilde{X}\,^2A_1/\tilde{A}\,^2B_2$ electronic character (>80% $\tilde{X}\,^2A_1$ character), $NO_2^{\ddagger}$ represents the TS, and the parent ground and excited states are labeled by the conserved representations of total spin–rovibronic symmetry (A_1,A_2), total angular momentum (J_0), and parity (P). In this picture, a single excited molecular eigenstate will project onto the manifold of fragment states via the vibrational levels of the TS. When one or more eigenstates overlap within their widths, they will be coherently excited and the resulting interference must be taken into account.

An examination of the NO_2 fluorescence excitation spectrum below D_0, which may be used as a lower bound estimation of the state density,[13] reveals a significant degree of congestion, with ~two rovibronic levels observed per cm^{-1}.[12] A larger density of states (~4 levels/cm^{-1}) has recently been determined from a higher resolution (i.e., 0.05 cm^{-1}) spectrum taken in the range 0–5 cm^{-1} below D_0.[49] However, as may be observed in the lower resolution spectra taken by the same workers,[12] this small region corresponds to a dense clump of transitions and thus may not accurately reflect the *average* state density above D_0. From real-time measurements of the decomposition rate,[13,14] we can estimate a linewidth contribution from lifetime broadening which ranges from <1 cm^{-1} near threshold to >20 cm^{-1} at $E^{\dagger}=2200$ cm^{-1}. Using the average rovibronic state density estimated from the lower resolution excitation spectrum, we note that the *average* decay width (>5 cm^{-1} for $E^{\dagger}>400$ cm^{-1}) is larger than the *average* spacing of the eigenstates ($\leqslant 0.5$ cm^{-1}) corresponding to the regime of overlapping resonances (i.e., $\langle\Gamma\rangle > \langle 1/\rho\rangle$). Visual comparisons of the recent high-resolution excitation spectrum obtained just below D_0 and the PHOFRY spectra obtained just above threshold by monitoring NO in J=0.5 and 1.5 (see Fig. 4 of Ref. 49) show clearly that the density of peaks actually *decreases* above threshold. Since the density of states does not abruptly diminish and many of the peaks above D_0 exhibit a substantial broadening with respect to the corresponding peaks below D_0, it is clear that the picture of overlapping resonances is valid even near threshold.

On the average, we expect to coherently excite several overlapped rovibronic resonances, which may interfere. As shown by Mies,[53] there is no simple relationship between the width of an observed resonance and the average decomposition lifetimes for overlapped eigenstates coupled to the same continuum. This is due to couplings among the eigenstates induced by their mutual interaction with the continuum, which give rise to shifts in peak positions as well as variations in their widths and shapes. As shown before,[53] the widths of the structures are determined by the phase angle, and narrow structures in absorption may appear even when the *average* decomposition lifetime is very short. The width of a resonance can be identified with a single-exponential decay rate only in the case of isolated resonances. We note that overlapping resonances were observed as asymmetric bands of varying width in the decomposition of formaldehyde.[35]

In addition to effects from overlapping resonances, the peaks observed in PHOFRY spectra may be broadened by incoherent superpositions and correlations among the states of the fragments. Due to incomplete rotational cooling in the jet (T_{rot}~5 K), incoherent excitation of levels originating from several rotational levels of NO_2 is possible, and the superposition of peaks may result in broadening. In addition, at excess energies above the thresholds for

formation of the higher spin–orbit states of oxygen, an average cross section into all $O(^3P_j)$ states is obtained even when monitoring a single NO state. Since the distribution of the $O(^3P_j)$ states correlated with a *single* NO state is unknown, these spectra cannot be deconvoluted. Recall that many of the PHOFRY spectra show peak positions and shapes that depend sensitively on the monitored product level. If each $NO(v,\Omega,\Lambda,J)+O(^3P_j)$ pair is associated with a slightly different PHOFRY spectrum for each $O(^3P_j)$ component, the observed peaks may be broadened by the summation over spectra corresponding to all $O(^3P_j)$ components. A clear example of this effect is revealed in the work of Miyawaki *et al.*,[12] who obtained PHOFRY spectra by monitoring a single $O(^3P_j)$ component, and thus summed over numerous $NO(v,\Omega,\Lambda,J)$ states. These spectra are much broader than those obtained in the present work by monitoring selected $NO(v,\Omega,\Lambda,J)$ states, each correlating with at most three $O(^3P_j)$ levels.

Due to effects from overlapping resonances, incoherent superpositions, and fragment correlations, one must view with skepticism the extraction of lifetime information from the widths of even isolated structures in state-selected PHOFRY spectra (see also Sec. IV C).

B. NO energy distributions, PHOFRY spectral correlations, and transition states

We now proceed to inspect more closely the product state distributions and, in particular, to examine how the fluctuations and oscillatory structures may yield information regarding the TS and its dependence on the NO degree of freedom and the excess energy. In a previous publication we concluded, based on the application of the SSE/PST method, that the vibrations in the NO fragment become adiabatic before rotations do so.[11] This result is confirmed by the observation that the fluctuation patterns in the rotational distributions of the two vibrational manifolds are uncorrelated (see Figs. 5 and 6 of Ref. 11 and Fig. 5), as well as by the very different PHOFRY spectra obtained when monitoring levels in the two vibrational manifolds (Figs. 9 and 10 and Ref. 45).

An intriguing correlation involves the similar oscillation patterns in the NO $^2\Pi_{1/2}$ and $^2\Pi_{3/2}$ rotational distributions observed at all excess energies examined (Figs. 3 and 4 and Ref. 11). This result is related to the strong correlation of the PHOFRY spectra of $^2\Pi_{1/2}(J)$, $^2\Pi_{3/2}(J-1)$ (i.e., the same N) pairs, and suggests that the NO rotational states become adiabatic before the spin–orbit state distribution is fixed. This is not surprising, since the $O(^3P)+NO(^2\Pi_{1/2},^2\Pi_{3/2})$ system has important long-range electrostatic interactions, such as the dipole–quadrupole and quadrupole–quadrupole, which may be important in inducing nonadiabatic transitions between different *asymptotic* fine-structure levels.[54] A comparison of the NO rotational distributions with PST predictions indeed suggests that long-range attractive forces are important in the $O(^3P)+NO(^2\Pi)$ system.[10,11] Nonadiabatic transitions between the surfaces correlating asymptotically with NO $^2\Pi_{1/2}$ and $^2\Pi_{3/2}$ may occur favorably at relatively large O–NO separations,[54] after the product rotational and vibrational states have become adiabatic. The dependence of the fluctuation patterns on N may reflect the weakness of the coupling of the NO electronic spin to either the NO internuclear axis [in Hund's case (a)], or to its rotational vector [in Hund's case (b)]. Thus, an external influence such as the fields associated with the adjacent oxygen atom may keep the spin decoupled from the NO nuclear and electronic degrees of freedom until the asymptotic region is reached, where the coupling of the spin to the NO nuclear and electronic coordinates determines its final spin–orbit state.

We observe NO $^2\Pi_{1/2}/^2\Pi_{3/2}$ ratios that are colder than statistical at all excess energies examined, with production of the $^2\Pi_{1/2}$ state consistently favored by a factor of ~ 3.[11] The spin–orbit state distribution of the $O(^3P_j)$ fragment at $E^\dagger \leqslant 2000$ cm^{-1} was also observed to be consistently colder than statistical, and in addition, the ratios oscillated with $E^\dagger$.[12] For the related $O(^3P)+OH(^2\Pi_{1/2,3/2})$ system, Graff and Wagner showed that at low collision energies, an adiabatic capture model results in smaller reaction cross sections for excited fine-structure surfaces,[54] since those surfaces are less attractive than the ground surface. Coupled with microscopic reversibility, the adiabatic correlations of the PESs for different asymptotic fine-structure levels suggest that cold spin–orbit distributions may in some cases be *inherently* expected, at least at low $E^\dagger$. We note that the largest energy gap between neighboring surfaces in the asymptotic region in NO_2 decomposition is that between the ground $[O(^3P_2)+NO(^2\Pi_{1/2})]$ and first excited $[O(^3P_2)+NO(^2\Pi_{3/2})]$ surfaces (123 cm^{-1}). If the ground surface is more attractive, this splitting would not decrease significantly (and indeed might increase) at shorter O–NO separations, making the probability for nonadiabatic transitions between the ground and excited fine structure surfaces relatively small and thus favoring a cold spin–orbit state distribution. We note that a quantitative prediction of the products' spin–orbit distributions is difficult since the long-range potentials are not well known and the final spin–orbit ratios may be determined by a combination of long-range electrostatic interactions, curve crossings, and interference effects.[55]

The oscillatory structures in the NO product state distributions can be understood by considering the scattering of molecular resonances into specific final states via the TS.[42,44] The PHOFRY spectra evidence fluctuations in the shapes, positions, and widths of the observed resonances, both when monitoring a single $NO(v,J,\Omega,\Lambda)$ level and when comparing spectra obtained by monitoring different levels.[10,11,16,45,49] The interference effects that may account for many of the observed spectral structures of varying widths and shapes (i.e., the resonances reflect the phases and the strengths of coupling of the overlapped molecular eigenstates)[53] are probably not responsible for the prominent structures in the rotational distributions. The excited molecule evolves into products in 5–0.2 ps at $E^\dagger < 3000$ cm^{-1} and, since some IVR has to occur for sufficient energy to accumulate in the reaction coordinate, the initial coherence that produces the observed resonances will be largely lost prior to dissociation. However, once at the TS,

the system must proceed to products on the time scale of a vibrational period, and therefore structures that originate at the TS are more likely to survive. For example, if the TS has levels with bending-like character, the mapping of these levels into angular momentum states of the products may produce oscillatory structures. Such structures have been predicted for fast dissociations[56–59] and observed experimentally in the photodissociation of CINO, FNO, and H_2O.[60,61] In these cases, a *single* TS wave function was expanded in terms of free rotor wave functions, and the rotational distributions exhibited oscillatory structures reminiscent of harmonic oscillator wave functions and their nodes.[59,61] In contrast, in unimolecular reactions, usually more than one TS level is populated and each fragment state can be formed via more than one zeroth-order wave function of the TS. This can lead to interference, resulting in additional structures and loss of correspondence between the observed oscillatory structures in the rotational distributions and a specific TS zeroth-order wave function.

Careful inspection of the patterns of fluctuations in the rotational distributions as a function of $E^\dagger$ reveals that for the majority of the $v=0$ and 1 distributions, the appearance of the structures changes qualitatively with increasing $E^\dagger$. Near their respective appearance thresholds, the distributions obtained for each NO Λ-doublet component are less structured and, following summation of the two Λ-doublet states, the fluctuations are largely suppressed and a reasonable agreement with PST is obtained.[11,16,49] This behavior is consistent with the suggestion that near the energetic threshold of *each* NO vibrational level, the TS is still very loose (i.e., PST-like) and can be described with a basis set of free-rotor wave functions. Mappings of such unhindered rotor wave functions will lead to a rather uniform sampling of phase space and less structured rotational distributions. However, when $E^\dagger$ is increased, larger oscillations are observed, which are not significantly diminished by summing over the different Λ-doublet components (see Fig. 5 and Ref. 11). When the TS tightens, mappings of its *bending-like* basis functions onto final rotational states may give rise to prominent structures and result in less uniform sampling of the available phase space. Thus, our results suggest that each fragment vibration evolves adiabatically, and the TS for each vibration becomes tighter as the excess energy increases. Notice also that each resonance in the PHOFRY spectrum, which is composed of several overlapping molecular eigenstates of highly mixed character, will project randomly onto the various accessible levels of the TS, and thus structures in the NO rotational distributions may vary greatly with small changes in photolysis wavelength; however, on the average, this random projection leads to statistical behavior.

We still need to explain why different peak positions and shapes are often observed in the PHOFRY spectra of different NO(v,J) levels, a behavior that has also been observed near D_0.[16,49] We suggest that the key is the different parentage of each NO final state, which may originate from a slightly different set of TS levels, in turn arising via projections from a different subset of overlapping molecular eigenstates. Since the position, shape, and width of the observed resonances depend on the number, amplitudes, and phases of the overlapping eigenstates that correlate with the monitored final state (i.e., continuum), it is not surprising that the spectra vary when different final states are monitored. However, similar J's may derive predominantly from a similar set of TS levels and therefore sample a similar set of molecular eigenstates. Therefore, their PHOFRY spectra will usually show greater similarities than those obtained when monitoring very different J's.

In summary, the interference among overlapping eigenstates increases IVR, since each resonance is an admixture of several already strongly mixed eigenstates. The random projection of these resonances onto the accessible TS levels may explain the success of statistical theories in describing, on the average, the NO product state distributions. However, mappings of TS wave functions, including the interferences resulting from projections through multiple TS levels into each final state, may be responsible for the fluctuations and oscillatory structures, and thus the deviations from statistical behavior.[11] The differences observed in the PHOFRY spectra of different NO(v,J) levels are ascribed to differences in the composition of the molecular eigenstates initially sampled, in that different final states sample a different set of molecular eigenstates whose interference gives rise to the different resonance structures seen in the PHOFRY spectra.

C. Comparisons to other results and implications to unimolecular reaction rates

The picture of NO_2 decomposition that emerges from the product state distributions and the PHOFRY spectra involves a TS that is very loose (PST-like) near the threshold for the formation of each NO(v) state, but tightens progressively as $E^\dagger$ increases. Such a picture is in accord with other unimolecular reactions proceeding without a barrier [e.g., $CH_2CO(S_0)$ and $NCNO(S_0)$],[1,2,4] where the dissociation rates agree with PST predictions near the threshold for each product vibration, but deviate at higher $E^\dagger$. As previously mentioned, real-time measurements of NO_2 decomposition rates by Wittig and co-workers agree with RRKM predictions and, in addition, reveal a step-like behavior of $k(E)$ vs $E^\dagger$ above threshold.[13] In that work, the steps (separated by ~ 100 cm^{-1}) were interpreted as the sequential opening of bending-like vibrational levels of the transition state. In contrast, Miyawaki *et al.* have recently observed NO($J=0.5$) high-resolution PHOFRY spectra at the threshold which appear to spectrally broaden when NO($J=1.5$) becomes energetically allowed, implying a very loose TS near threshold (i.e., the TS levels can be described as NO free-rotor states).[49] This is not surprising, since a behavior that agrees with PST has been observed in $CH_2CO(S_0)$ dissociation near threshold by using time independent methods,[2] while time-resolved measurements showed deviations from PST at $E^\dagger > 70$ cm^{-1}.[4] In NCNO, another molecule that dissociates without a barrier, the agreement of time-resolved measurements with PST persists for several hundred wave numbers above D_0.[4] Thus, previous results on molecules dissociating without a barrier

show that the TS tightens with increasing energy, but the degree of tightening is apparently controlled by the shape of the PES. The steps observed in the real-time measurements of NO_2 may thus indicate that the TS moves in very quickly with increasing energy. This interpretation agrees with recent variational RRKM calculations on NO_2 that show step-size increases of the rates, with the energy difference between the steps increasing rapidly with increasing $E^\dagger$.[15]

It should, however, be noted that the *absolute* value of the decay rate depends sensitively on the value chosen for the density of states above D_0. Any uncertainty in this number will influence comparisons with statistical theories. Spectroscopic studies below D_0 show that the number of observed transitions is not uniform as a function of wavelength, and such nonuniformity will affect the rates and may cause some nonmonotonic behavior as a function of photolysis wavelength. Miyawaki *et al.* propose that the first step observed in the real time measurements at $E^\dagger \sim 100$ cm^{-1} arises from the opening of the excited NO spin–orbit state ($^2\Pi_{3/2}$).[49] However, we have previously shown that the spin–orbit state distribution of the NO fragment is relatively constant and remarkably *cold* over the energy range $E^\dagger$=0–3000 cm^{-1}, with the ground $^2\Pi_{1/2}$ state preferred by a factor of $\sim$3.[11] Therefore, it appears unlikely that the doubling of the rate measured at the first step can be attributed to the opening of this minor channel.

A more general issue concerns the time-dependent behavior of dissociating molecules in the regime of overlapping resonances and, in particular, the extraction of time-domain information from widths of resonances in the frequency domain. When overlapped resonances are excited, single-exponential decay rates may not be obtained. Whether the *average* decay rate obtained in the regime of overlapped resonances conforms to the RRKM rate is still an open question[62] and should be the subject of further experimental and theoretical scrutiny. In particular, narrow features may represent "entrapment" of excitation energy in the bound region due to recrossings and couplings to other bound states via a common continuum,[44,62] and broad resonances may give rise to a continuum-like background. Linewidths are usually extracted from narrow resonances, and consequently an average rate *smaller* than the RRKM value may be obtained. Also, as discussed previously, the linewidths observed in PHOFRY spectra of specific NO (v,J,Λ,Ω) states may be broadened by incoherent superposition of lines correlating with the three O(^3P_j) states and/or originating from several parent rotational levels. High-resolution PHOFRY studies using double-resonance excitation schemes are currently in progress in our lab in order to further address some of these issues.[45,63]

V. SUMMARY AND CONCLUSIONS

This paper examines fluctuations in the unimolecular reaction of NO_2, a simple bond-fission reaction that proceeds without a barrier following excitation of *overlapped resonances*. In particular, it emphasizes the implications of fluctuations in the NO rotational distributions and in line positions, widths, and shapes in the PHOFRY spectra to the mechanism of decomposition of NO_2. The results are discussed within the framework of statistical theories.[1,2,5,8,32,36,44] The main observations and conclusions are:

(1) The rotational distributions in each NO(v) state show marked oscillatory structures that become more prominent at higher excess energies. The magnitude and shapes of these oscillatory structures vary randomly with $E^\dagger$, and there is no correlation among structures obtained in v=0 and 1. No propensity for the formation of one Λ-doublet state is observed, and summation over the population of the two Λ-doublet components does not quench the fluctuations, especially at higher $E^\dagger$.

(2) Rotational distributions obtained in the two NO spin–orbit states, $^2\Pi_{1/2}$ and $^2\Pi_{3/2}$, show similar oscillatory structures, especially when plotted as a function of $N=J \pm 1/2$. This similarity is also evidenced in the similar PHOFRY spectra obtained by monitoring NO $^2\Pi_{1/2}$ and $^2\Pi_{3/2}$ levels of the same N.

(3) The PHOFRY spectra exhibit resonances arising from coherent excitation of overlapping molecular eigenstates. These resonances have shapes and widths that vary with $E^\dagger$; in addition, the peak positions, shapes, and widths of the resonances depend on the monitored NO rovibrational level. Interference effects, incoherent superpositions of lines, and fragment correlations must be taken into account when attempting to extract lifetimes from the widths of these spectral features.

(4) Despite their differences, some PHOFRY spectra show distinct correlations. Spectra obtained by monitoring NO states of similar angular momentum within each vibrational manifold are strongly correlated, and a good correlation is also observed when monitoring levels of $^2\Pi_{1/2}(J)$ and $^2\Pi_{3/2}(J-1)$ (i.e., the same N) as described above. This indicates that NO levels of similar angular momentum are correlated with similar sets of resonances [see also item (6)]. In addition, some subtle correlations based on parity may exist.

(5) Our results suggest that the NO vibrational states first become adiabatic, followed by the rotational, and last, the electronic degrees of freedom. A tightening of the rotational TS with increasing $E^\dagger$ is also suggested, and the evolution of bending-like TS basis wave functions, excited coherently, into product rotations may be responsible for the oscillatory structures in the NO rotational distributions. The good agreement obtained on the average with the predictions of statistical theories is a manifestation of the highly mixed nature of the excited resonances and their random projections onto levels of the TS.

(6) We suggest that the dependence of the resonance peak positions and widths on the monitored NO level in the PHOFRY spectra may be related to the different set of coherently overlapping molecular eigenstates that is correlated with each monitored NO(v,J) state. More work is needed to understand and describe quantitatively the effects due to overlapping resonances.

To conclude, we should mention under what conditions fluctuations might be expected in unimolecular decompositions. Several important conditions, such as mo-

noenergetic excitation, few initial parent levels, and few available final states, have been identified previously. While these conditions are certainly fulfilled in our experiment, other studies of unimolecular decompositions of jet-cooled molecules, such as NCNO (Ref. 1) and ketene (Ref. 2), have also largely satisfied these conditions, yet fluctuations in the product state distributions are not noticeable. NO_2, with a small density of states, but highly mixed molecular eigenstates due to strong vibronic coupling, may fundamentally represent the transition point between statistical and dynamical behavior. The observation of dynamical effects in NO_2 is no doubt helped by the inherent correlation of rovibronic states of the $NO(^2\Pi_\Omega;\ \Omega=1/2,3/2)$ fragment with only three levels, the spin–orbit states, of the $O(^3P_j;\ j=2,1,0)$ fragment. Indeed, fluctuations of a similar nature have also been observed in the CO rotational distributions following the 157.6 nm photolysis of CO_2.[10,30] However, for the uni-molecular decomposition of NCNO which produces two diatoms, correlations among the numerous available states of the fragments are expected to significantly dampen such fluctuations, and may explain why they are not observed in that system. In addition, the higher level density of a system such as NCNO ($\rho_{vib}\sim 250$ per cm^{-1} near threshold) may average out the fluctuations to a level not detectable experimentally.

Note added in proof. After this paper was submitted, H. Katagiri and S. Kato [J. Chem. Phys. **99**, 8805 (1993)] reported a calculated of the NO spin–orbit state distribution in the photodissociation of NO_2. Their calculated $^2\Pi_{3/2}/^2\Pi_{1/2}$ ratio of 0.29 for $J=3$ is remarkably close to our experimental value of ~ 0.3.

ACKNOWLEDGMENTS

The authors wish to thank M. Hunter for assistance in obtaining and analyzing the data shown in Figs. 2–5; C. Wittig, S. Ionov, H. S. Taylor, and R. W. Shaw for many useful discussions; and J. Pfab and P. Houston for sending preprints of their work on NO_2. This research is supported by the National Science Foundation and the U. S. Army Research Office.

[1] C. X. W. Qian, M. Noble, I. Nadler, H. Reisler, and C. Wittig, J. Chem. Phys. **83**, 5573 (1985); H. Reisler and C. Wittig, Annu. Rev. Phys. Chem. **37**, 307 (1986) and references therein; in *Advances in Chemical Kinetics and Dynamics*, edited by J. R. Barker (JAI, Greenwich, CT, 1992), Vol. 1, p. 139.

[2] I.-C. Chen, W. H. Green, Jr., and C. B. Moore, J. Chem. Phys. **89**, 314 (1988); W. H. Green, Jr., I.-C. Chen, and C. B. Moore, Ber. Bunsenges. Phys. Chem. **92**, 389 (1988); W. H. Green, Jr., C. B. Moore, and W. F. Polik, Annu. Rev. Phys. Chem. **43**, 307 (1992), and references therein.

[3] L. J. Butler, T. M. Ticich, M. D. Likar, and F. F. Crim, J. Chem. Phys. **85**, 2331 (1986); T. M. Ticich, T. R. Rizzo, H. R. Dübal, and F. F. Crim, *ibid.* **84**, 1508 (1986).

[4] L. R. Khundkar, J. L. Knee, and A. H. Zewail, J. Chem. Phys. **87**, 77 (1987); S. J. Klippenstein, L. R. Khundkar, A. H. Zewail, and R. A. Marcus, *ibid.* **89**, 4761 (1988); S. J. Klippenstein and R. A. Marcus, *ibid.* **91**, 2280 (1989).

[5] (a) P. Pechukas, J. C. Light, and C. Rankin, J. Chem. Phys. **44**, 794 (1966); (b) P. Pechukas and J. C. Light, *ibid.* **42**, 3281 (1965); (c) J. C. Light, Discuss. Faraday Soc. **44**, 14 (1967).

[6] J. T. Yardley, *Introduction to Molecular Energy Transfer* (Academic, New York, 1980).

[7] C. Wittig, I. Nadler, H. Reisler, J. Catanzarite, and G. Radhakrishnan, J. Chem. Phys. **83**, 5581 (1985).

[8] (a) D. M. Warlaw and R. A. Marcus, Chem. Phys. Lett. **110**, 230 (1984); (b) J. Chem. Phys. **83**, 3462 (1985); (c) Adv. Chem. Phys. **70**, 231 (1988).

[9] (a) D. J. Nesbitt, H. Petek, M. F. Foltz, S. V. Filseth, D. J. Bamford, and C. B. Moore, J. Chem. Phys. **83**, 223 (1985); (b) W. H. Green, Jr., A. J. Mahoney, Q.- K. Zheng, and C. B. Moore, *ibid.* **94**, 196 (1991).

[10] D. C. Robie, M. A. Hunter, J. L. Bates, and H. Reisler, Chem. Phys. Lett. **192**, 279 (1992).

[11] M. A. Hunter, S. A. Reid, D. C. Robie, and H. Reisler, J. Chem. Phys. **99**, 1093 (1993).

[12] J. Miyawaki, K. Yamanouchi, and S. Tsuchiya, Chem. Phys. Lett. **180**, 287 (1991).

[13] (a) G. A. Brucker, S. I. Ionov, Y. Chen, and C. Wittig, Chem. Phys. Lett. **194**, 301 (1992); (b) S. I. Ionov, G. A. Brucker, C. Jaques, Y. Chen, and C. Wittig, J. Chem. Phys. **99**, 3420 (1993).

[14] (a) J. Troe, Ber. Bunsenges. Phys. Chem. **73**, 144 (1969); (b) **73**, 906 (1969); (c) H. Gaedtke and J. Troe, *ibid.* **77**, 24 (1973); (d) M. Quack and J. Troe, *ibid.* **78**, 240 (1974).

[15] S. J. Klippenstein and T. Radivoyevitch, J. Chem. Phys. **99**, 3644 (1993).

[16] (a) U. Robra, H. Zacharias, and K. Welge, Z. Phys. D **16**, 175 (1990); (b) U. Robra, Ph.D. thesis, 1984.

[17] C. H. Chen, D. W. Clark, M. G. Payne, and S. D. Kramer, Opt. Commun. **32**, 391 (1980).

[18] T. J. Butenhoff and E. A. Rohlfing, J. Chem. Phys. **98**, 5460 (1993).

[19] A. E. Douglas, J. Chem. Phys. **45**, 1007 (1966).

[20] (a) E. Haller, H. Köppel, and L. S. Cederbaum, J. Mol. Spectrosc. **111**, 377 (1985); (b) H. Köppel, W. Domcke, and L. S. Cederbaum, Adv. Chem. Phys. **57**, 59 (1984).

[21] K. K. Lehmann and S. L. Coy, Ber. Bunsenges. Phys. Chem. **92**, 306 (1988).

[22] A. Delon and R. Jost, J. Chem. Phys. **95**, 5686 (1991).

[23] A. Delon, R. Jost, and M. Lombardi, J. Chem. Phys. **95**, 5701 (1991).

[24] C. F. Jackels and E. R. Davidson, J. Chem. Phys. **64**, 2908 (1976).

[25] C. F. Jackels and E. R. Davidson, J. Chem. Phys. **65**, 2941 (1976).

[26] G. D. Gillespie and A. U. Khan, J. Chem. Phys. **65**, 1624 (1976).

[27] G. D. Gillespie, A. U. Kahn, A. C. Wahl, R. P. Hosteny, and M. Krauss, J. Chem. Phys. **63**, 3425 (1975).

[28] L. Burnelle, A. M. May, and R. A. Gangi, J. Chem. Phys. **49**, 561 (1968); (b) R. A. Gangi and L. Burnelle, *ibid.* **55**, 851 (1971).

[29] J. L. Hardwick, J. Mol. Spectrosc. **109**, 85 (1985).

[30] R. L. Miller, S. H. Kable, P. L. Houston, and I. Burak, J. Chem. Phys. **96**, 32 (1992).

[31] L. Bigio and E. R. Grant, J. Chem. Phys. **87**, 360 (1987).

[32] (a) W. H. Miller, R. Hernandez, C. B. Moore, and W. F. Pollik, J. Chem. Phys. **93**, 5657 (1990); (b) R. Hernandez, W. H. Miller, C. B. Moore, and W. F. Polik, *ibid.* **99**, 950 (1993).

[33] W. F. Polik, D. R. Guyer, and C. B. Moore, J. Chem. Phys. **92**, 3453 (1990).

[34] W. F. Polik, D. R. Guyer, W. H. Miller, and C. B. Moore, J. Chem. Phys. **92**, 3471 (1990).

[35] W. F. Polik, C. B. Moore, and W. H. Miller, J. Chem. Phys. **89**, 3584 (1988).

[36] R. D. van Zee, C. D. Pibel, T. J. Butenhoff, and C. B. Moore, J. Chem. Phys. **97**, 3235 (1992).

[37] G. R. Satchler, *Introduction to Nuclear Reactions* (Oxford University, New York, 1990), pp. 252–256.

[38] T. Ericson, Ann. Phys. **23**, 390 (1963).

[39] I. Rotter, Rep. Prog. Phys. **54**, 635 (1991).

[40] T. Ericson, Phys. Rev. Lett. **5**, 430 (1960).

[41] K. J. Laidler, *Theories of Chemical Reaction Rates* (McGraw–Hill, New York, 1979).

[42] (a) F. H. Mies, J. Chem. Phys. **51**, 787 (1969); (b) **51**, 798 (1969).

[43] (a) G. G. Hall and R. D. Levine, J. Chem. Phys. **44**, 1567 (1966); (b) R. D. Levine, *ibid.* **44**, 2029 (1966); **44**, 2035 (1966); **44**, 2046 (1966); (c) *Quantum Mechanics of Molecular Rate Processes* (Oxford University, Oxford, 1969).

[44] F. H. Mies and M. Krauss, J. Chem. Phys. **45**, 4455 (1966).

[45] S. A. Reid, J. T. Brandon, M. A. Hunter, and H. Reisler, J. Chem. Phys. **99**, 4860 (1993).

[46] C. X. W. Qian, A. Ogai, L. Iwata, and H. Reisler, J. Chem. Phys. **92**, 4296 (1990).

[47] I. Deézi, Acta Phys. Hungary **9**, 125 (1958).
[48] R. D. Bower, R. W. Jones, and P. L. Houston, J. Chem. Phys. **79**, 2799 (1983).
[49] J. Miyawaki, K. Yamanouchi, and S. Tsuchiya, J. Chem. Phys. **99**, 254 (1993).
[50] N. Changlong, L. Hua, and J. Pfab, J. Phys. Chem. **97**, 7458 (1993).
[51] P. Andresen and E. W. Rothe, J. Chem. Phys. **82**, 3634 (1985).
[52] R. W. Shaw, Jr., J. C. Norman, R. Vandenbosch, and C. J. Bishop, Phys. Rev. **184**, 1040 (1968).
[53] F. H. Mies, Phys. Rev. **175**, 164 (1968).
[54] M. M. Graff and A. F. Wagner, J. Chem. Phys. **92**, 2423 (1990).
[55] (a) M. H. Alexander, J. Chem. Phys. **92**, 337 (1985); (b) **85**, 5652 (1986).
[56] C. X. W. Qian, A. Ogai, J. Brandon, Y. Y. Bai, and H. Reisler, J. Phys. Chem. **95**, 6763 (1991).
[57] (a) M. D. Morse and K. F. Freed, J. Chem. Phys. **74**, 4395 (1981); (b) **78**, 6045 (1983); (c) Chem. Phys. Lett. **74**, 49 (1980).
[58] (a) M. D. Morse, K. F. Freed, and Y. B. Band, J. Chem. Phys. **70**, 3604 (1979); (b) **70**, 3620 (1979).
[59] (a) R. Schinke, A. Untch, H. U. Suter, and J. R. Huber, J. Chem. Phys. **94**, 7929 (1991); (b) R. Schinke, *Photodissociation Dynamics* (Cambridge University, Cambridge, 1993).
[60] R. Schinke, R. L. Vander Wal, J. L. Scott, and F. F. Crim, J. Chem. Phys. **94**, 283 (1991).
[61] A. Ogai, J. Brandon, H. Reisler, H. U. Suter, J. R. Huber, M. Von Dirke, and R. Schinke, J. Chem. Phys. **96**, 6643 (1992).
[62] M. Desouter-Lecomto and F. Culot, J. Chem. Phys. **98**, 7819 (1993).
[63] S. A. Reid and H. Reisler (unpublished).